HHS Public Access

Author manuscript

Ultrasound Med Biol. Author manuscript; available in PMC 2021 October 01.

Published in final edited form as:

Ultrasound Med Biol. 2020 October ; 46(10): 2625–2635. doi:10.1016/j.ultrasmedbio.2020.06.009.

Visualization of microvascular angiogenesis using dual-frequency contrast enhanced acoustic angiography: a review

Isabel G. Newsome[a], **Paul A. Dayton**[a,*]

[a]Joint Department of Biomedical Engineering, University of North Carolina at Chapel Hill and North Carolina State University, Chapel Hill, NC, USA

Abstract

Cancerous tumor growth is associated with the development of tortuous, chaotic microvasculature, and this aberrant microvascular morphology can act as a biomarker of malignant disease. Acoustic angiography is a contrast-enhanced ultrasound technique that relies on superharmonic imaging to form high-resolution, three-dimensional maps of the microvasculature. To date, acoustic angiography has been performed with dual-element transducers that can achieve high contrast-to-tissue ratio and resolution in preclinical small animal models. In this review, we first describe the development of acoustic angiography, including the principle, transducer design, and optimization of superharmonic imaging techniques. We then detail several preclinical applications of this microvascular imaging method, as well as the current and future development of acoustic angiography as a preclinical and clinical diagnostic tool.

Keywords

ultrasound; microbubbles; contrast agent; angiography; angiogenesis; microvasculature

Introduction

Microvasculature in Cancer

Many diseases, such as cancer, are affected by aberrant microvasculature. To fuel their rapid growth, tumors induce angiogenesis, the formation of new blood vessels from pre-existing vasculature, by overexpressing pro-angiogenic factors (Folkman 1971; Jain 2001). This tumor-associated neovascularization is considered one of the “hallmarks of cancer” (Hanahan and Weinberg 2011) and results in vascular structures that differ greatly from those seen in healthy tissue – vessels are highly tortuous, leaky, disorganized, and densely packed, rather than linear and well organized (Jain 2001). The structural and functional abnormality observed in this microvasculature leads to increased interstitial pressure, acidosis, and hypoxia, which contribute in part to the difficulty of effectively treating cancer (Jain 2005). It is this observation that has motivated the development of anti-angiogenic

*Corresponding author: padayton@email.unc.edu, 1-919-966-1175, 116 Manning Dr, CB 7575, Chapel Hill, NC, 27599.

Conflict of Interest

P.A.D. declares that he is an inventor on a patent describing dual-frequency imaging and a co-founder of SonoVol, Inc., which has licensed this patent and manufactures imaging systems with acoustic angiography capability.

therapies in an attempt to “normalize” the vasculature and hence improve treatment efficacy (Jain 2005).

Angiogenesis may serve as a biomarker of malignant disease as well as a therapeutic target. The increased microvascular density and tortuosity observed in and surrounding cancerous tumors might be used as both qualitative and quantitative metrics in the detection and diagnosis of these lesions. In order for this to be achieved, a diagnostic method must be able to image these vascular features with high resolution in three dimensions (3D).

Biomedical Imaging of Vasculature

In the clinic, angiography, or blood vessel imaging, is traditionally performed as computed tomography (CT) angiography or magnetic resonance (MR) angiography (Wu et al. 2016). Though these modalities allow vascular imaging in three dimensions, they both present limitations when considered as tools for screening and monitoring disease progression or response to therapy. CT requires the use of ionizing radiation, while MR is costly and time-intensive, and both modalities have limited resolution (~700 μm with the best currently approved clinical systems) (Pinker et al. 2014; Reiner et al. 2013). Neither imaging modality is highly portable nor low cost, especially in relation to the next generation of handheld ultrasound systems. As such, there is a clinical need for high-resolution, safe, accessible vascular imaging. Ultrasound is arguably the safest, cheapest, and most available form of biomedical imaging beyond planar x-ray, and with Doppler processing techniques or the addition of microbubble contrast agents (MCAs), ultrasound can be used to image blood flow (Bercoff et al. 2011; Klibanov and Hossack 2015). However, these vascular imaging techniques suffer from poor sensitivity due to the presence of tissue background, limited resolution, and inability to image slow-flowing vessels. To address these limitations, superharmonic imaging can be utilized to produce high-resolution, high-contrast microvascular images. In this review, we introduce the ultrasound principles behind this technique and discuss optimization, applications, and future directions of a superharmonic technique, known as acoustic angiography.

Development of Acoustic Angiography

Superharmonic Ultrasound Imaging

Superharmonic imaging is a variant of traditional ultrasound imaging that employs a strategy for separating signals from tissue and contrast agents based on the superharmonic content of microbubble echoes. In conventional “B-mode” ultrasound, an acoustic wave with a specific frequency (typically 1 – 10 MHz for clinical use) is transmitted into tissue from the transducer (Noce 1990; Rizzatto 1998). As the wave propagates into tissue, portions are reflected back to the transducer, and these received echoes are processed to form an ultrasound image. At low acoustic pressures, the energy contained in these tissue echoes is concentrated at the fundamental frequency (same as the transmit frequency), whereas only a small portion of energy is contained within the harmonic frequencies (higher multiples of the transmit frequency). Although nonlinear propagation of the acoustic wave causes more energy to shift to the harmonics as the transmitted acoustic pressure is increased, this effect

is small at typical parameters used for contrast imaging (Rizzatto 1998; Tranquart et al. 1999).

In contrast, MCAs behave quite differently than tissue under acoustic stimulation. Typical microbubbles are composed of a high molecular weight gas core encapsulated by a lipid, protein, or polymer shell (Ferrara et al. 2007). Due to their highly compressible core, MCAs oscillate when exposed to ultrasound waves, producing broadband echoes which span multiples of the fundamental frequency (De Jong et al. 2002; Ferrara et al. 2007). The echoes generated at the third harmonic and above (i.e. ≥ 3x the fundamental frequency) are known as the "superharmonic" microbubble response (Bouakaz et al. 2002). By selectively receiving these higher frequency signals, superharmonic imaging can achieve better resolution and contrast-to-tissue ratio (CTR) than conventional B-mode or other contrast-enhanced ultrasound imaging techniques, which largely rely on detecting bubbles by second harmonic signal (Bouakaz et al. 2002; Kruse and Ferrara 2005). Increased resolution is provided by the higher frequencies detected, and improved CTR is due to the fact that tissue produces minimal superharmonic content.

However, implementing superharmonic imaging effectively requires non-traditional transducer technology, as conventional ultrasound transducers have limited bandwidth, meaning they cannot effectively transmit and receive signals at both the fundamental and higher order harmonic frequencies. To achieve the necessary bandwidth for this technique, transducers with completely independent elements for excitation and reception are typically used. Figure 1a provides an idealistic illustration of this dual-frequency approach to superharmonic imaging in the frequency domain. In some previous studies, phased arrays have been designed with interleaved transmit and receive elements (Bouakaz et al. 2002; van Neer et al. 2010). Using one such transducer with 0.8 MHz transmit and 2.9 MHz receive, Bouakaz *et al.* (2003) demonstrated high CTR with superharmonic imaging compared to second harmonic imaging in human contrast-enhanced echocardiography. Others have implemented confocal dual-element transducers *in vitro* (Guiroy et al. 2013; Kruse and Ferrara 2005). Kruse and Ferrara (2005) performed superharmonic M-mode imaging with confocal pistons at 2.25 and 15 MHz for transmit and receive, respectively, while Guiroy *et al.* (2013) designed a confocal device with 4 MHz transmit and 14 MHz receive and imaged in 2D by raster-scanning the transducer over the imaging target.

Implementation and Optimization of Acoustic Angiography

Acoustic angiography is a technique that applies superharmonic imaging in three dimensions to form volumetric maps of microvascular structures. Similar to the works mentioned above, acoustic angiography to date has employed confocal dual-element transducers, comprised of a high-frequency central element surrounded by a low-frequency annular element, as shown in Fig. 1b (Gessner et al. 2010), allowing complete isolation of the excitation and reception bandwidths. These transducers are used to perform superharmonic imaging with 2 – 4 MHz transmit on one transducer element and 25 – 30 MHz receive on the second element (Gessner et al. 2010; Gessner et al. 2013). The transducer elements are mechanically scanned on a motor-controlled arm, or "wobbler," to form a two-dimensional image (Foster et al. 2000). Acoustic angiography was initially performed with these custom transducers

(modified RMV scanheads, FUJIFILM VisualSonics, Inc., Toronto, ON, Canada) and a preclinical high-frequency ultrasound system (Vevo 770, FUJIFILM VisualSonics, Inc., Toronto, ON, Canada). High-frequency B-mode and reception during dual-frequency imaging is controlled by this scanner, while low-frequency transmit is controlled by an arbitrary waveform generator (AWG2021, Tektronix, Inc., Beaverton, OR, USA) and power amplifier (model 240L, Electronics & Innovation, Ltd., Rochester, NY, USA). The dual-frequency wobbler probes used for acoustic angiography have a fixed focal depth of 13 – 16 mm and depth of field of approximately 8 – 12 mm. To acquire three-dimensional images, the transducer is translated on a linear motion stage. A schematic of the acoustic angiography imaging setup is shown in Fig. 1c.

With this system, acoustic angiography can resolve vessels on the order of 150 – 200 μm and CTR on the order of 20 dB *in vivo* (Gessner et al. 2013; Lindsey et al. 2014; Lindsey et al. 2015b). Figure 2 provides example images of a subcutaneous fibrosarcoma tumor in a rat flank, including a high frequency B-mode image (a), the corresponding 2D acoustic angiography slice (b), and three representations of the volumetric acoustic angiography dataset, including the dual-frequency image stack (c), a 3D rendering of the volume (d), and a maximum intensity projection (MIP) through depth (e).

The amount of superharmonic signal generated by MCAs depends on both acoustic parameters of the excitation and characteristics of the microbubbles themselves (De Jong et al. 2002), while the receive frequency bandwidth determines imaging depth, resolution, and sensitivity. Lindsey *et al.* (2014) have studied the superharmonic response, examining CTR and resolution for various combinations of excitation frequency, pressure, and receive frequency. Their results indicated that CTR is maximized for excitation frequencies between 1.5 – 3.5 MHz and reception frequencies between 10 – 15 MHz and confirmed that receive frequency is primarily responsible for determining resolution (Lindsey et al. 2014).

In a following study, Lindsey and colleagues (2015a) went on to explore the mechanism behind broadband superharmonic generation at various excitation frequencies and pressures. The authors found that the strongest signals were produced at high pressures that also resulted in microbubble fragmentation, although weaker superharmonic signals could be produced at pressures that were not immediately destructive to bubbles and usually correlated with slow bubble deflation or destruction over multiple pulses (Lindsey et al. 2015a). This study demonstrated the importance of balancing excitation pressure and frame rate in order to maintain contrast signal throughout imaging. This effect is illustrated in Fig. 3, which shows acoustic angiography MIPs of a subcutaneous fibrosarcoma tumor in a rat flank collected with two different pressures. At 1200 kPa, microbubble destruction is dominant, resulting in an image of larger, fast flowing microvessels (Fig. 3a). At 560 kPa, microbubbles persist through many pulses, emphasizing slow flowing microvasculature (Fig. 3b). It should be noted that the larger vessels are captured in both cases. Because the images are displayed as MIPs through depth and there is relatively less signal at 560 kPa, the signal from the larger vessels is buried beneath the capillaries closer to the transducer in Fig. 3b. Lindsey *et al.* (2015b) also showed that the shape of the low-frequency transmit pulse can be optimized for improved CTR in acoustic angiography.

The studies described in the previous paragraphs all focused on optimizing the acoustic parameters used for acoustic angiography, but our group has also begun examining how microbubble parameters may affect this imaging technique. Newsome *et al.* (2019b) performed a comprehensive evaluation of superharmonic signal generation by 14 different MCAs when excited with pressures between 400 – 2400 kPa at 4 MHz. The authors illustrated that microbubble characteristics, such as shell composition and bubble diameter, have an effect on superharmonic production (Newsome et al. 2019b). Future works will continue to study the interplay of acoustic and microbubble parameters in acoustic angiography imaging.

Applications of Acoustic Angiography

To date, acoustic angiography has been used to image microvasculature in a variety of preclinical studies. In order for acoustic angiography to be an appropriate tool, the anatomy of interest should be within several centimeters from the skin surface, the target must be perfused with MCAs, and effective acoustic coupling must be applied. The sections below discuss several notable applications of acoustic angiography.

Evaluating Microvascular Morphology

As mentioned previously, vascular morphology is altered in the presence of malignant tumors, resulting in highly tortuous vessels. Tortuosity metrics, such as the sum-of-angles metric and the distance metric (Bullitt et al. 2003), can be used to quantify the morphology of the microvasculature. Before this quantitative analysis, vessels must first be segmented from the image volume (Aylward and Bullitt 2002).

Morphological analysis has been performed in various small animal cancer models with acoustic angiography. Gessner *et al.* (2012) collected acoustic angiography images from healthy and tumor-bearing tissue in a subcutaneous rat fibrosarcoma model and found significantly higher tortuosity in tumor-bearing compared to healthy tissue, suggesting that this form of quantitative analysis may be able to differentiate tumors from normal tissue (Fig. 4). Shelton *et al.* (2015) went on to use acoustic angiography to monitor angiogenesis throughout tumor development in a spontaneous murine model of breast cancer. In this work, the authors showed that tumor microvasculature is significantly more tortuous than that of healthy tissue, even early in development when tumors are as small as 2 mm (Shelton et al. 2015). In a following study, through analysis of B-mode images, which reflect tissue anatomy, as well as microvascular acoustic angiography images, Rao *et al.* (2016) examined the location of tortuous vessels feeding solid tumors and observed that cancer-associated angiogenesis extended beyond what is typically considered the boundaries of solid tumors. Shelton *et al.* (Shelton et al. 2020) then showed that tumors on the order of 5 mm in diameter could be detected with high specificity and sensitivity through both qualitative and quantitative analysis of acoustic angiography images in a murine model of breast cancer. These studies demonstrated that acoustic angiography, followed by visual assessment, microvascular segmentation, and morphological analysis, can provide insight into vascular biomarkers of tumor growth and progression and has the potential to improve diagnostic accuracy in clinical cancer care.

Imaging Molecular Markers of Angiogenesis

Ultrasound molecular imaging is a functional contrast-enhanced ultrasound technique that employs MCAs that are targeted to biological markers, resulting in images depicting the distribution of a specific molecular target (Abou-Elkacem et al. 2015; Bachawal et al. 2013; Streeter et al. 2010; Tsuruta et al. 2017). This imaging technique typically employs multi-pulse, second harmonic contrast-enhanced ultrasound. Previous work from our group has implemented molecular imaging in combination with acoustic angiography, providing high resolution vascular information to better understand biomarker distribution evaluated with ultrasound molecular imaging (Lindsey et al. 2017b; Shelton et al. 2016).

Shelton *et al.* (2016) first demonstrated the feasibility of superharmonic molecular imaging, showing that the dual-frequency strategy used for acoustic angiography can detect microbubbles bound to $\alpha_v\beta_3$ integrin, a factor involved in tumor-associated angiogenesis, *in vivo* in a subcutaneous rat fibrosarcoma model. Lindsey *et al.* (2017b) went on to compare superharmonic molecular imaging to traditional ultrasound molecular imaging in the same tumor model. The authors showed that superharmonic molecular imaging, in combination with microvascular imaging, provided greater CTR than conventional molecular imaging (Lindsey et al. 2017b). Acoustic angiography was combined with superharmonic molecular imaging of angiogenic (VEGFR2) and inflammatory (P- and E-selectins) targeted bubbles to illustrate both biomarker distribution and tumor microvasculature, as shown in Fig. 5. These studies demonstrated that the spatial information provided by microvascular acoustic angiography data, such as distance from targeted signal to the nearest vessel and nearby vessel tortuosity, could potentially be used for quantitative analysis of molecular imaging (Lindsey et al. 2017b; Shelton et al. 2016).

Monitoring Response to Therapy

As previously mentioned, anti-angiogenic therapy can be used to negatively affect or even halt the development of angiogenesis as a treatment for some cancers. The effects of such therapy on the microvasculature can be evaluated with acoustic angiography. With a SonoVol Vega™ system, described previously by Czernuszewicz and colleagues (2018), Rojas *et al.* (2018) used acoustic angiography to monitor tumor response to anti-angiogenic treatment in a murine model of renal cell carcinoma. Specifically, the authors quantified response to therapy by measuring vascular density from acoustic angiography images, and the vascular density metric showed significance one week earlier than tumor volume in this rodent model (Rojas et al. 2018). This work illustrated the potential of acoustic angiography as a tool for monitoring response to therapy more effectively than current standards, such as tumor volume, and future studies will continue to assess this technique with other cancer and treatment models.

Validating Preclinical Research Models

The high-resolution 3D microvascular information provided by acoustic angiography makes this imaging technique an exceptional tool for non-invasive validation of experimental models. Some previous studies have used acoustic angiography as a comparison to other novel imaging techniques (Mohanty et al. 2019; Panfilova et al. 2019). Mohanty *et al.* (2019) used acoustic angiography to confirm that measurement of multiple scattering from

intravascular microbubbles is related to vessel density and that this metric can be used to differentiate tumors from healthy tissue. Panfilova *et al.* (2019) explored the role of microvascular architecture on the results of dynamic contrast-enhanced ultrasound by comparing metrics derived from acoustic angiography, such as vascular density and tortuosity, to metrics derived from dynamic contrast-enhanced ultrasound, such as perfusion and dispersion. Other work has employed acoustic angiography as a means of validating the presence of functional vasculature (Dunleavey et al. 2014; Wahl et al. 2019). Dunleavey *et al.* (2014) used acoustic angiography to assess *in vivo* formation and function of vascular structures in melanoma tumors dependent on adhesion molecule expression, while Wahl *et al.* (2019) employed acoustic angiography to verify vascular integration of human lung implants in a humanized mouse model (Fig. 6). Overall, these studies demonstrate the versatility of acoustic angiography as a non-invasive microvascular imaging tool in preclinical research.

Future Directions of Acoustic Angiography

Imaging Breast Cancer with Acoustic Angiography

The preclinical studies described in the previous sections demonstrate the potential of acoustic angiography as a diagnostic imaging tool for cancer. Because the high receive frequency limits the penetration depth of acoustic angiography, human cancers that develop shallow tumors are ideal targets for this technique. One such target is breast cancer. Breast cancer is the most prevalent cancer in women, with an incidence rate of 12.5% in the United States (Noone et al. 2018), and current diagnostic imaging for breast cancer suffers from poor specificity. Standard of care breast screening relies on mammography for the identification of suspicious lesions, but approximately 20% of women who have an abnormal screening result undergo biopsy, and more than 65% of these biopsies are benign (Seely and Alhassan 2018; Weaver et al. 2006). These unnecessary biopsies are estimated to cost upward of $2 billion annually in the United States alone (Vlahiotis et al. 2018), in addition to the physical and psychological stress experienced by these patients. These statistics serve to emphasize a current dearth of high specificity diagnostic breast imaging modalities. By combining microvascular information with standard ultrasound data, acoustic angiography may be able to help fill this void and improve the standard of care for women with suspicious breast lesions.

Recently, the first human acoustic angiography data was published by Shelton *et al.* (2017). The authors showed that acoustic angiography with dual-frequency wobbler transducers was able to resolve vessels as small as 200 μm in human breast (Shelton et al. 2017). However, this pilot study also elucidated several limitations of the current acoustic angiography technology. Imaging depth was significantly limited by the fixed focus, shallow field of view, and high receive frequency of the prototype dual-frequency wobbler used in the study, such that only lesions within 1.5 cm of the skin surface could be imaged (Shelton et al. 2017). Severe artifacts were introduced by respiration motion due to the relatively slow data acquisition required for the mechanical steering of the transducer elements (Shelton et al. 2017). In addition, clinical images exhibited reduced sensitivity (i.e. CTR) compared to preclinical acoustic angiography images due to restrictions in MCA dose allowed in clinical

patients (Shelton et al. 2017). Overall, these challenges indicated that dual-frequency transducer technology for acoustic angiography must be improved for effective clinical microvascular ultrasound imaging with this technique.

Typically, clinical ultrasound imaging is performed with array transducers, which offer many benefits over single-element transducers, including faster data acquisition, deeper and more flexible imaging through electronic focusing, and improved image quality with advanced imaging schemes and post-processing techniques. It follows that the next generation of dual-frequency transducers for improved clinical acoustic angiography will be array transducers. However, designing dual-frequency array transducers is technically challenging. A recent study by Cherin *et al.* (2019) utilized a hybrid dual-frequency device, which consisted of a commercial high-frequency array with a prototype two-element transducer for superharmonic imaging, in a similar configuration to previous colinear transducers designed by others (Stephens et al. 2006; Stephens et al. 2008; Zheng et al. 2008). The authors demonstrated high CTR in a phantom with 1.7 MHz transmit and 20 MHz receive on this hybrid probe (Cherin et al. 2019). Kierski *et al.* (Kierski et al. 2020) have since employed this hybrid design for fast-frame-rate plane-wave acoustic angiography, followed by ultrasound localization microscopy processing, producing super-resolved images of *in vivo* rodent microvasculature. It is worth noting that the array configuration enabled sufficient sensitivity that superharmonic imaging could be performed at very low mechanical indices, less than 0.3. The advantage of combining acoustic angiography with super-resolution processing is that it eliminates the need for spatiotemporal filtering and can be sensitive to slow contrast flow which can confound filters, such as singular value decomposition (Kierski et al. 2020). Furthermore, this combination approach may enable performing high resolution microvascular imaging at much lower frequencies than previously used in acoustic angiography, enabling penetration to deep tissues, but recovering the high resolution through super-resolution processing, and retaining robustness to slow flow in the presence of tissue motion.

With devices such as this hybrid format bridging the gap between single-element and array transducers, our group will continue to develop the acoustic angiography technique for clinical translation, including optimization of transmit and receive frequencies, transducer configurations, and MCA parameters. Future work will focus on the development of integrated coaxial dual-frequency arrays for clinical microvascular imaging at depth. One such array has been developed using a novel stacked design, consisting of a 2 MHz linear array coaxially stacked behind a 20 MHz linear array (Newsome et al. 2019a). Preliminary work with this dual-frequency array has shown an improvement in sensitivity over dual-frequency wobbler transducers and resolution on the order of 200 μm *in vivo* (Newsome et al. 2019a).

Other Transducer Technologies for Acoustic Angiography

The works described in the previous sections have all utilized dual-frequency transducers placed externally on the body. However, intracavity and intravascular applications of acoustic angiography have also been explored by our group and collaborators. To facilitate microvascular assessment of deep, difficult to image prostate tumors with acoustic

angiography, Li *et al.* (2018) described a colinear dual-frequency array which was tested up to 4 cm in depth *in vitro* and successfully detected microvasculature *in vivo* in a rodent model. Similarly, Lindsey *et al.* (2017a) demonstrated the feasibility of acoustic angiography imaging with a dual-frequency endoscopic transducer for pancreatic cancer evaluation with high CTR up to 3 cm depth *in vitro*.

Aside from cancer, acoustic angiography may be useful in other diseases with unique microvascular features, such as atherosclerosis and cardiovascular disease. In atherosclerosis, vulnerable plaques are characterized by pathological infiltration of the vasa vasorum (microvasculature that feeds the adventitia in large arteries) through the vessel wall and into the plaque itself (Martin et al. 2016). While assessment of the vasa vasorum may improve diagnosis of cardiovascular disease (Mantella et al. 2019), these microvessels are difficult to image due to their small size and anatomical position. Consequently, Martin *et al.* (2016) and Wang *et al.* (2018) developed dual-frequency catheter-based ultrasound probes designed for intravascular imaging of the *vasa vasorum*, showing high sensitivity and resolution in both *ex vivo* and *in vitro* vascular models.

Finally, while the current bandwidth limitations of piezoelectric devices have required the use of multi-frequency transducers for superharmonic imaging, an alternative technology that may lend itself to this application is the capacitive micromachined ultrasonic transducer (CMUT). CMUTs are microfabricated devices that can be produced with a greater bandwidth than piezoelectric transducers and may provide an alternative solution to achieve the ultra-wide bandwidth needed for acoustic angiography. CMUTs have been previously utilized for ultra-wideband imaging of other multi-frequency events, such as acoustic droplet vaporization (Novell et al. 2016), although they have inherent nonlinear behavior that requires extra processing to separate transmitted content from that scattered by microbubbles (Novell et al. 2015).

Alternative Angiographic Ultrasound Methods

While we have focused on acoustic angiography in this review, there are many other ultrasound methods that can be used to image microvasculature. The following paragraphs briefly summarize a few such techniques, but it should be noted that more comprehensive reviews have been published elsewhere (Christensen-Jeffries et al. 2020; Demené et al. 2019; Hu and Wang 2010; Jiang et al. 2019).

Doppler-based ultrasound techniques are commonly used in clinical patient care. While these methods do not require contrast injection, they can suffer from poor spatial or temporal resolution (Bercoff et al. 2011). Recent advances in acquisition and processing have led to the development of new Doppler-based modalities, such as superb microvascular imaging (Jiang et al. 2019) and ultrafast Doppler imaging (Bercoff et al. 2011). These techniques can image and provide functional information for vessels greater than 100 μm in diameter without the administration of contrast (Demené et al. 2019). However, Doppler methods require repeated acoustic interrogation of the same imaging plane, which significantly increases acquisition time.

Inspired by advances in optical imaging, ultrasound localization microscopy (ULM) forms images by localizing individual microbubbles over thousands of consecutive frames to populate the vascular tree (Christensen-Jeffries et al. 2020). Since the introduction of ULM, countless groups have adapted this novel technique, highlighting the extraordinary ability of ULM to image vessels with resolution as fine as 10 μm(Christensen-Jeffries et al. 2020). However, ULM acquisition requires considerable time to populate the smallest vessels in a region of interest, and image processing requires significant computational power and time. Furthermore, ULM is highly sensitive to tissue motion due to the long acquisition times.

Photoacoustic imaging methods rely on the photoacoustic effect, a physical phenomenon in which an object produces acoustic waves when irradiated with optical energy (Hu and Wang 2010). This effect is exhibited by hemoglobin in the bloodstream, allowing angiographic imaging without exogenous contrast (Hu and Wang 2010). Photoacoustic techniques can range from photoacoustic microscopy with 5 μm resolution and up to 1 mm penetration depth to photoacoustic computed tomography with 500 μm resolution and up to 50 mm penetration depth (Hu and Wang 2010; Yao and Wang 2013). Acoustic angiography has previously been compared to photoacoustic imaging by Gessner and colleagues (Gessner et al. 2013).

To summarize, there are many approaches to vascular imaging with ultrasound, including the techniques described in this section and the myriad others that have been described elsewhere. Some methods are excellent tools for deep imaging but can suffer from poor resolution, such as Doppler-based approaches (Demené et al. 2019) and clinical contrast-enhanced ultrasound (Wilson et al. 2020). Other techniques, such as acoustic angiography and photoacoustic tomography (Hu and Wang 2010), can provide high resolution in shallow applications, while ultrasound localization microscopy offers the potential for high resolution imaging of microvasculature at depth (Christensen-Jeffries et al. 2020).

Conclusion

Acoustic angiography is a non-invasive, three-dimensional, contrast-enhanced ultrasound technique that enables high-resolution imaging of microvasculature. Microvascular imaging may provide preclinical and clinical utility for a multitude of applications, from assessing microvascular disease biomarkers, to monitoring therapy, to validating research models. Although this imaging technology is largely limited by challenges in designing optimized hardware, continued development of dual-frequency transducer technology will facilitate the translation of this technique into the clinic.

Acknowledgements

All studies cited in this review received approval from their respective Institutional Animal Care and Use Committees or Institutional Review Boards for studies involving animal or human subjects, respectively.

The described work would not have been possible without the efforts of many collaborators who appear as co-authors in the works cited here, not only from the University of North Carolina at Chapel Hill but also from the University of Toronto, North Carolina State University, FUJIFILM Visualsonics, Inc., and Kitware, Inc. The authors wish to thank the National Institutes of Health for financial support of this research program through R01 CA170665, R01 CA170665S1, R01 EB026897, R01 CA189479, R44 CA165621, and R01 EB015508. I.G.N. has been partially supported in her training through National Institutes of Health Grants T32 HL069768 and F31

CA24317. Additional funding has been supplied by the Department of Defense through project W81XWH-12-1-0303, as well as from UNC Lineberger Comprehensive Cancer Center pilot grants.

References

Abou-Elkacem L, Bachawal SV, Willmann JK. Ultrasound Molecular Imaging: Moving Towards Clinical Translation. Eur J Radiol 2015;84:1685–1693. [PubMed: 25851932]

Aylward SR, Bullitt E. Initialization, noise, singularities, and scale in height ridge traversal for tubular object centerline extraction. IEEE Trans Med Imaging 2002;21:61–75. [PubMed: 11929106]

Bachawal SV, Jensen KC, Lutz AM, Gambhir SS, Tranquart F, Tian L, Willmann JK. Earlier Detection of Breast Cancer with Ultrasound Molecular Imaging in a Transgenic Mouse Model. Cancer Res 2013;73:1689–1698. [PubMed: 23328585]

Bercoff J, Montaldo G, Loupas T, Savery D, Mézière F, Fink M, Tanter M. Ultrafast compound doppler imaging: Providing full blood flow characterization. IEEE Trans Ultrason Ferroelectr Freq Control 2011;58:134–147. [PubMed: 21244981]

Bouakaz A, Frigstad S, Ten Cate FJ, Jong NDE. SUPER HARMONIC IMAGING: A NEW IMAGING TECHNIQUE FOR IMPROVED CONTRAST DETECTION. Ultrasound Med Biol 2002;28:59–68. [PubMed: 11879953]

Bouakaz A, Krenning BJ, Vletter WB, Ten Cate FJ, De Jong N. Contrast superharmonic imaging: A feasibility study. Ultrasound Med Biol 2003;29:547–553. [PubMed: 12749924]

Bullitt E, Gerig G, Pizer SM, Lin W, Aylward SR. Measuring Tortuosity of the Intracerebral Vasculature from MRA Images. IEEE Trans Med Imaging 2003;22:1163–1171. [PubMed: 12956271]

Cherin E, Yin J, Forbrich A, White C, Dayton PA, Foster FS, Démoré CEM. In Vitro Superharmonic Contrast Imaging Using a Hybrid Dual-Frequency Probe. Ultrasound Med Biol 2019;45:2525–2539. [PubMed: 31196746]

Christensen-Jeffries K, Couture O, Dayton PA, Eldar YC, Hynynen K, Kiessling F, O'Reilly M, Pinton GF, Schmitz G, Tang MX, Tanter M, van Sloun RJG. Super-resolution Ultrasound Imaging. Ultrasound Med Biol 2020;46:865–891. [PubMed: 31973952]

Czernuszewicz TJ, Papadopoulou V, Rojas JD, Rajamahendiran RM, Perdomo J, Butler J, Harlacher M, O'Connell G, Zukić D, Aylward SR, Dayton PA, Gessner RC. A new preclinical ultrasound platform for widefield 3D imaging of rodents. Rev Sci Instrum 2018;89.

De Jong N, Bouakaz A, Frinking P. Basic acoustic properties of microbubbles. Echocardiography 2002;19:229–240. [PubMed: 12022933]

Demené C, Mairesse J, Baranger J, Tanter M, Baud O. Ultrafast Doppler for neonatal brain imaging. Neuroimage 2019;185:851–856. [PubMed: 29649559]

Dunleavey JM, Xiao L, Thompson J, Kim MM, Shields JM, Shelton SE, Irvin DM, Brings VE, Ollila DW, Brekken RA, Dayton PA, Melero-Martin JM, Dudley AC. Vascular channels formed by subpopulations of PECAM1 þ melanoma cells. Nat Commun 2014;5.

Ferrara K, Pollard R, Borden M. Ultrasound Microbubble Contrast Agents: Fundamentals and Application to Gene and Drug Delivery. Annu Rev Biomed Eng 2007;9:415–47. [PubMed: 17651012]

Folkman J Tumor Angiogenesis: Therapeutic Implications. N Engl J Med 1971;285:1182–1186. [PubMed: 4938153]

Foster FS, Pavlin CJ, Harasiewicz KA, Christopher DA, Turnbull DH. Advances in ultrasound biomicroscopy. Ultrasound Med Biol 2000;26:1–27. [PubMed: 10687788]

Gessner R, Lukacs M, Lee M, Cherin E, Foster FS, Dayton PA. High-Resolution, High-Contrast Ultrasound Imaging Using a Prototype Dual-Frequency Transducer : In Vitro and In Vivo Studies. IEEE Trans Ultrason Ferroelectr Freq Control 2010;57:1772–1781. [PubMed: 20679006]

Gessner RC, Aylward SR, Dayton PA. Mapping Microvasculature with Acoustic Angiography Yields Quantifiable Differences between Healthy and Tumor-bearing Tissue Volumes in a Rodent Model. Radiology 2012;264:733–740. [PubMed: 22771882]

Gessner RC, Frederick CB, Foster FS, Dayton PA. Acoustic Angiography: A New Imaging Modality for Assessing Microvasculature Architecture. Int J Biomed Imaging 2013;936593. [PubMed: 23997762]

Guiroy A, Novell A, Ringgaard E, Lou-Moeller R, Grégoire JM, Abellard AP, Zawada T, Bouakaz A, Levassort F. Dual-frequency transducer for nonlinear contrast agent imaging. IEEE Trans Ultrason Ferroelectr Freq Control 2013;60:2634–2644. [PubMed: 24297028]

Hanahan D, Weinberg RA. Hallmarks of Cancer: The Next Generation. Cell 2011;144:646–674. [PubMed: 21376230]

Hu S, Wang LV. Photoacoustic imaging and characterization of the microvasculature. J Biomed Opt 2010;15:011101. [PubMed: 20210427]

Jain RK. Normalizing tumor vasculature with anti-angiogenic therapy: A new paradigm for combination therapy. Nat Med 2001;7:987–989. [PubMed: 11533692]

Jain RK. Normalization of tumor vasculature : An emerging concept in angiogenic therapy. Science (80-) 2005;307:58–62.

zhen Jiang Z, hua Huang Y, liang Shen H, tian Liu X. Clinical Applications of Superb Microvascular Imaging in the Liver, Breast, Thyroid, Skeletal Muscle, and Carotid Plaques. J Ultrasound Med 2019;38:2811–2820. [PubMed: 30953387]

Kierski TM, Espindola D, Newsome IG, Cherin E, Yin J, Foster FS, Demore CEM, Pinton GF, Dayton PA. Super harmonic ultrasound for motion-independent localization microscopy: applications to microvascular imaging from low to high flow rates. IEEE Trans Ultrason Ferroelectr Freq Control 2020;67:957–967. [PubMed: 31940529]

Klibanov AL, Hossack JA. Ultrasound in Radiology: from Anatomic, Functional, Molecular Imaging to Drug Delivery and Image-Guided Therapy. Invest Radiol 2015;50:657–670. [PubMed: 26200224]

Kruse DE, Ferrara KW. A new imaging strategy using wideband transient response of ultrasound contrast agents. IEEE Trans Ultrason Ferroelectr Freq Control 2005;52:1320–1329. [PubMed: 16245601]

Li S, Kim J, Wang Z, Kasoji S, Lindsey BD, Dayton PA, Jiang X. A dual-frequency colinear array for acoustic angiography in prostate cancer evaluation. IEEE Trans Ultrason Ferroelectr Freq Control IEEE, 2018;65:2418–2428.

Lindsey BD, Kim J, Dayton PA, Jiang X. Dual-Frequency Piezoelectric Endoscopic Transducer for Imaging Vascular Invasion in Pancreatic Cancer. IEEE Trans Ultrason Ferroelectr Freq Control 2017a;64:1078–1086. [PubMed: 28489536]

Lindsey BD, Rojas JD, Dayton PA. On the Relationship Between Microbubble Fragmentation, Deflation and Broadband Superharmonic Signal Production. Ultrasound Med Biol 2015a;41:1711–1725. [PubMed: 25766572]

Lindsey BD, Rojas JD, Martin KH, Shelton SE, Dayton PA. Acoustic characterization of contrast-to-tissue ratio and axial resolution dual-frequency contrast-specific acoustic angiography imaging. IEEE Trans Ultrason Ferroelec, Freq Contr 2014;61:1668–1687.

Lindsey BD, Shelton SE, Dayton PA. OPTIMIZATION OF CONTRAST-TO-TISSUE RATIO THROUGH PULSE WINDOWING IN DUAL-FREQUENCY "'ACOUSTIC ANGIOGRAPHY'" IMAGING. Ultrasound Med Biol 2015b;41:1884–1895. [PubMed: 25819467]

Lindsey BD, Shelton SE, Foster FS, Dayton PA. Assessment of Molecular Acoustic Angiography for Combined Microvascular and Molecular Imaging in Preclinical Tumor Models. Mol Imaging Biol 2017b;19:194–202. [PubMed: 27519522]

Mantella LE, Colledanchise KN, Hétu M-F, Feinstein SB, Abunassar J, Johri AM. Carotid intraplaque neovascularization predicts coronary artery disease and cardiovascular events. Eur Hear J - Cardiovasc Imaging 2019;1:1–9.

Martin KH, Lindsey BD, Ma J, Nichols TC, Jiang X, Dayton PA. Ex Vivo Porcine Arterial and Chorioallantoic Membrane Acoustic Angiography Using Dual-Frequency Intravascular Ultrasound Probes. Ultrasound Med Biol 2016;42:2294–2307. [PubMed: 27260246]

Mohanty K, Papadopoulou V, Newsome IG, Shelton S, Dayton PA, Muller M. Ultrasound multiple scattering with microbubbles can differentiate between tumor and healthy tissue in vivo. Phys Med Biol 2019;64.

Newsome IG, Kierski TM, Carnevale C, Visualsonics F, Cherin E, Foster FS. Enhanced Depth of Field Acoustic Angiography with a Prototype 288-element Dual-Frequency Array. Proc - IEEE Int Ultrason Symp 2019a.

Newsome IG, Kierski TM, Dayton PA. Assessment of the Superharmonic Response of Microbubble Contrast Agents for Acoustic Angiography as a Function of Microbubble Parameters. Ultrasound Med Biol 2019b;45:2515–2524. [PubMed: 31174922]

Noce JP. Fundamentals of diagnostic ultrasonography. Biomed Instrum Technol 1990;24:456–459. [PubMed: 2261584]

Noone AM, Howlader N, Krapcho M, Miller D, Brest A, Yu M, Ruhl J, Tatalovich Z, Mariotto A, Lewis DR, Chen HS, Feuer EJ, Cronin KA. SEER Cancer Statistics Review, 1975–2015. Bethesda, MD, 2018.

Novell A, Arena CB, Kasoji S, Dayton PA. Optimization of multi-pulse sequences for nonlinear contrast agent imaging using a cMUT array. Phys Med Biol 2015;60.

Novell A, Arena CB, Oralkan O, Dayton PA. Wideband acoustic activation and detection of droplet vaporization events using a capacitive micromachined ultrasonic transducer. J Acoust Soc Am 2016;139:3193–3198. [PubMed: 27369143]

Panfilova A, Shelton SE, Caresio C, van Sloun RJG, Molinari F, Wijkstra H, Dayton PA, Mischi M. On the Relationship between Dynamic Contrast-Enhanced Ultrasound Parameters and the Underlying Vascular Architecture Extracted from Acoustic Angiography. Ultrasound Med Biol 2019;45:539–548. [PubMed: 30509785]

Pinker K, Bogner W, Baltzer P, Trattnig S, Gruber S, Abeyakoon O, Bernathova M, Zaric O, Dubsky P, Bago-Horvath Z, Weber M, Leithner D, Helbich TH. Clinical application of bilateral high temporal and spatial resolution dynamic contrast-enhanced magnetic resonance imaging of the breast at 7 T. Eur Radiol 2014;24:913–920. [PubMed: 24306425]

Rao SR, Shelton SE, Dayton PA. The “Fingerprint” of Cancer Extends Beyond Solid Tumor Boundaries: Assessment With a Novel Ultrasound Imaging Approach. IEEE Trans Biomed Eng 2016;63:1082–1086. [PubMed: 26394410]

Reiner CS, Roessle M, Thiesler T, Eberli D, Klotz E, Frauenfelder T, Sulser T, Moch H, Alkadhi H. Computed Tomography Perfusion Imaging of Renal Cell Carcinoma. Invest Radiol 2013;48:1. [PubMed: 23070097]

Rizzatto G Ultrasound Transducers. Eur J Radiol 1998;27:S188–S195. [PubMed: 9652521]

Rojas JD, Papadopoulou V, Czernuszewicz T, Rajamahendiran R, Chytil A, Chiang Y-C, Chong D, Bautch V, Rathmell K, Aylward S, Gessner R, Dayton PA. Ultrasound Measurement of Vascular Density to Evaluate Response to Anti-angiogenic Therapy in Renal Cell Carcinoma. IEEE Trans Biomed Eng 2018;PP:1–1.

Seely JM, Alhassan T. Screening for breast cancer in 2018—what should we be doing today? Curr Oncol 2018;25:S115–S124. [PubMed: 29910654]

Shelton SE, Lee YZ, Lee M, Cherin E, Foster FS, Aylward SR, Dayton PA. Quantification of microvascular tortuosity during tumor evolution using acoustic angiography. Ultrasound Med Biol 2015;41:1896–1904. [PubMed: 25858001]

Shelton SE, Lindsey BD, Dayton PA, Lee YZ. First-in-Human Study of Acoustic Angiography in the Breast and Peripheral Vasculature. Ultrasound Med Biol 2017;43:2939–2946. [PubMed: 28982628]

Shelton SE, Lindsey BD, Tsuruta JK, Foster FS, Dayton PA. MOLECULAR ACOUSTIC ANGIOGRAPHY: A NEW TECHNIQUE FOR HIGH-RESOLUTION SUPERHARMONIC ULTRASOUND MOLECULAR IMAGING. Ultrasound Med Biol 2016;42:769–781. [PubMed: 26678155]

Shelton SE, Stone J, Gao F, Zeng D, Dayton PA. Microvascular Ultrasonic Imaging of Angiogenesis Identifies Tumors in a Murine Spontaneous Breast Cancer Model. Int J Biomed Imaging 2020;7862089. [PubMed: 32089667]

Stephens DN, Kruse DE, Ergun AS, Barnes S, Lu XM, Ferrara KW. Efficient array design for sonotherapy. Phys Med Biol 2008;53:3943–3969. [PubMed: 18591737]

Stephens DN, Lu XM, Proulx T, Walters W, Dayton P, Tartis M, Kruse DE, Lum AFH, Kitano T, Stieger SM, Ferrara K. Multi-frequency array development for drug delivery therapies:

Characterization and first use of a triple row ultrasound probe. Proc - IEEE Ultrason Symp 2006;1:66–69.

Streeter J, Gessner R, Miles I, Dayton PA. Improving Sensitivity in Ultrasound Molecular Imaging by Tailoring Contrast Agent Size Distribution: In Vivo Studies. Mol Imaging 2010;9:87–95. [PubMed: 20236606]

Tranquart F, Grenier N, Eder V, Pourcelot L. Clinical Use of Ultrasound Tissue Harmonic Imaging. Ultrasound Med Biol 1999;25:889–894. [PubMed: 10461715]

Tsuruta JK, Schaub NP, Rojas JD, Streeter J, Klauber-DeMore N, Dayton P. Optimizing ultrasound molecular imaging of secreted frizzled related protein 2 expression in angiosarcoma. PLoS One 2017;12:e0174281. [PubMed: 28333964]

van Neer PLMJ, Matte G, Danilouchkine MG, de Jong N, Prins C, van den Adel F. Super-Harmonic Imaging: Development of an Interleaved Phased-Array Transducer. IEEE Trans Ultrason Ferroelectr Freq Control 2010;57:455–468. [PubMed: 20178912]

Vlahiotis A, Griffin B, Stavros AT, Margolis J. Analysis of utilization patterns and associated costs of the breast imaging and diagnostic procedures after screening mammography. Clin Outcomes Res 2018;10:157–167.

Wahl A, De C, Abad Fernandez M, Lenarcic EM, Xu Y, Cockrell AS, Cleary RA, Johnson CE, Schramm NJ, Rank LM, Newsome IG, Vincent HA, Sanders W, Aguilera-Sandoval CR, Boone A, Hildebrand WH, Dayton PA, Baric RS, Pickles RJ, Braunstein M, Moorman NJ, Goonetilleke N, Victor Garcia J. Precision mouse models with expanded tropism for human pathogens. Nat Biotechnol 2019;37:1163–1173. [PubMed: 31451733]

Wang Z, Martin KH, Dayton PA, Jiang X. Real-time ultrasound angiography using superharmonic dual-frequency (2.25 MHz/30 MHz) cylindrical array: In vitro study. Ultrasonics 2018;82:298–303. [PubMed: 28941396]

Weaver DL, Rosenberg RD, Barlow WE, Ichikawa L, Carney PA, Kerlikowske K, Buist DSM, Geller BM, Key CR, Maygarden SJ, Ballard-Barbash R. Pathologic findings from the breast cancer surveillance consortium: Population-based outcomes in women undergoing biopsy after screening mammography. Cancer 2006;106:732–742. [PubMed: 16411214]

Wilson SR, Burns PN, Kono Y. Contrast-Enhanced Ultrasound of Focal Liver Masses: A Success Story. Ultrasound Med Biol 2020;46:1059–1070. [PubMed: 32059917]

Wu G, Yang J, Zhang T, Morelli JN, Giri S, Li X, Tang W. The diagnostic value of non-contrast enhanced quiescent interval single shot (QISS) magnetic resonance angiography at 3T for lower extremity peripheral arterial disease, in comparison to CT angiography. J Cardiovasc Magn Reson 2016;18.

Yao J, Wang LV. Photoacoustic Microscopy. Laser Photon Rev 2013;7.

Zheng H, Kruse DE, Stephens DN, Ferrara KW, Sutcliffe P, Gardner E. A sensitive ultrasonic imaging method for targeted contrast microbubble detection. Proc 30th Annu Int Conf IEEE Eng Med Biol Soc EMBS'08 - "Personalized Healthc through Technol 2008 pp. 5290–5293.

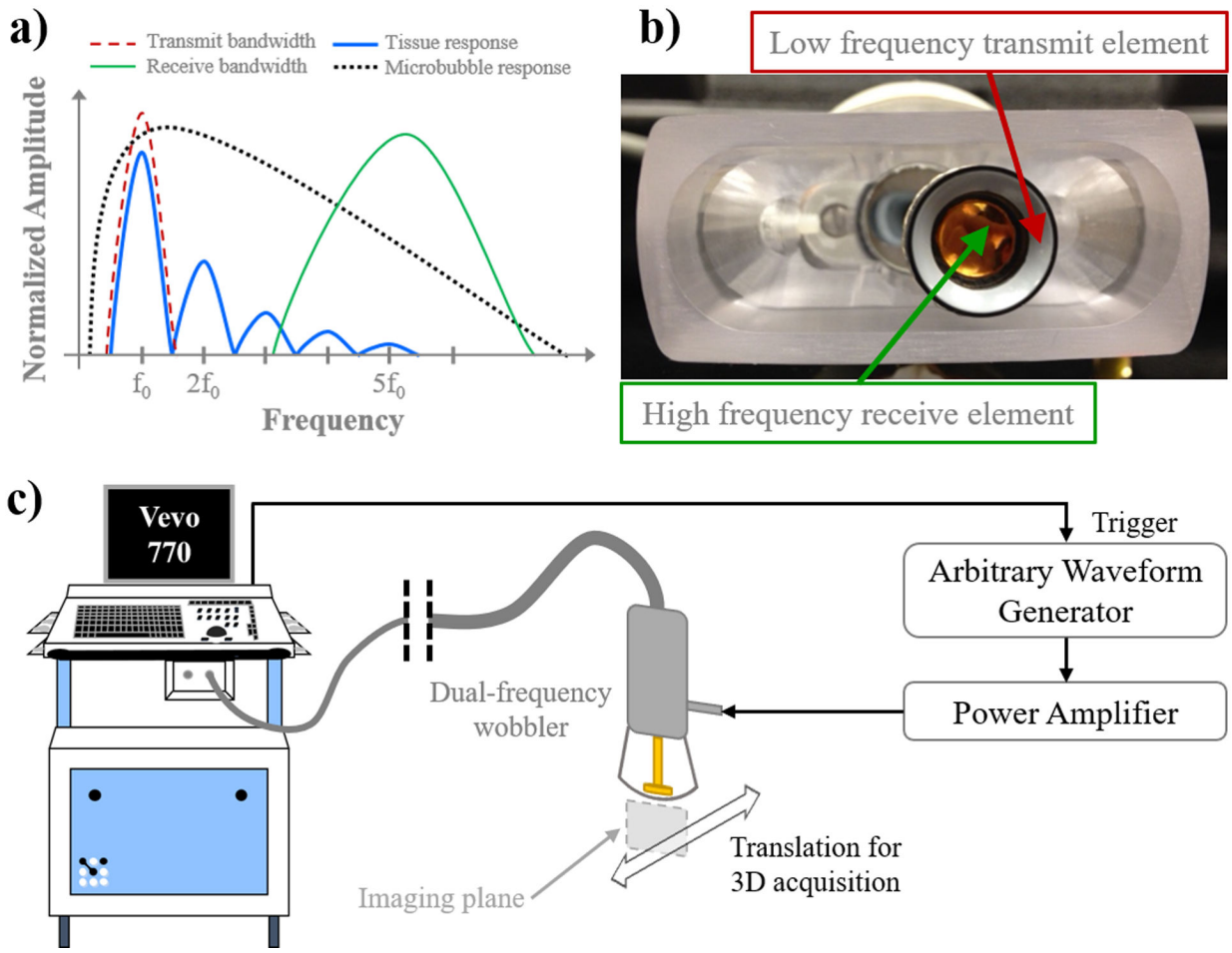

Figure 1:

a) Description of the acoustic angiography technique in the frequency domain, b) example of a dual-frequency wobbler transducer, and c) schematic diagram of the acoustic angiography imaging setup.

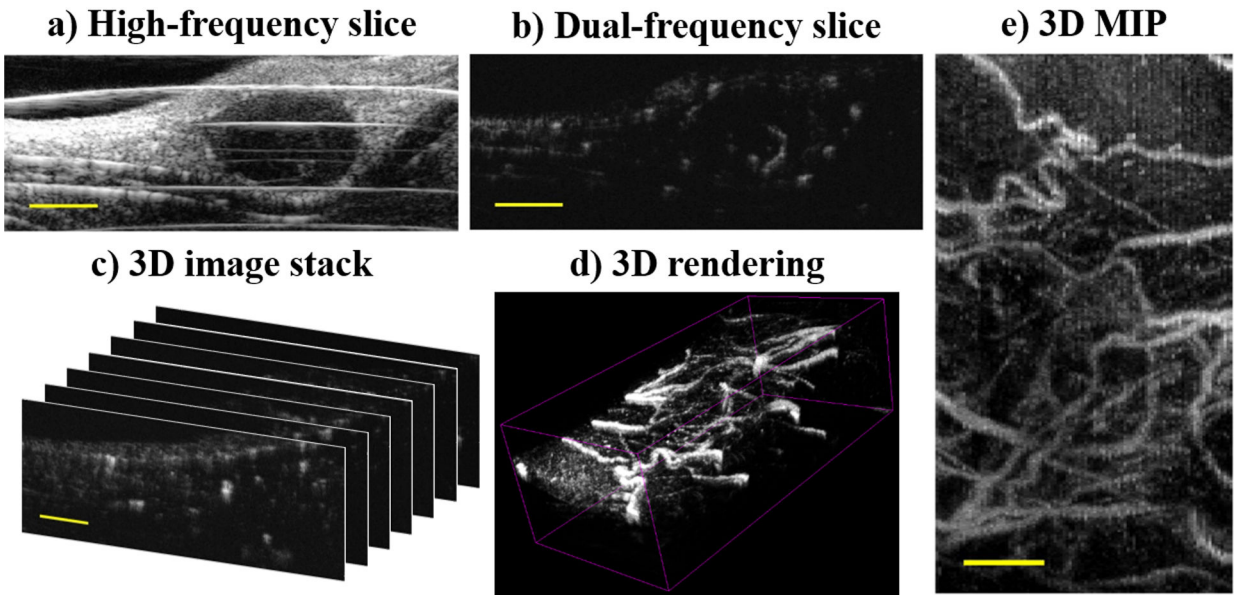

Figure 2:
Example images of a subcutaneous rat fibrosarcoma tumor: a) high-frequency B-mode, b) 2D acoustic angiography slice, c) 3D acoustic angiography image stack, d) volumetric rendering of (c), and e) maximum intensity projection (MIP) of (c). Scale bar = 3 mm.

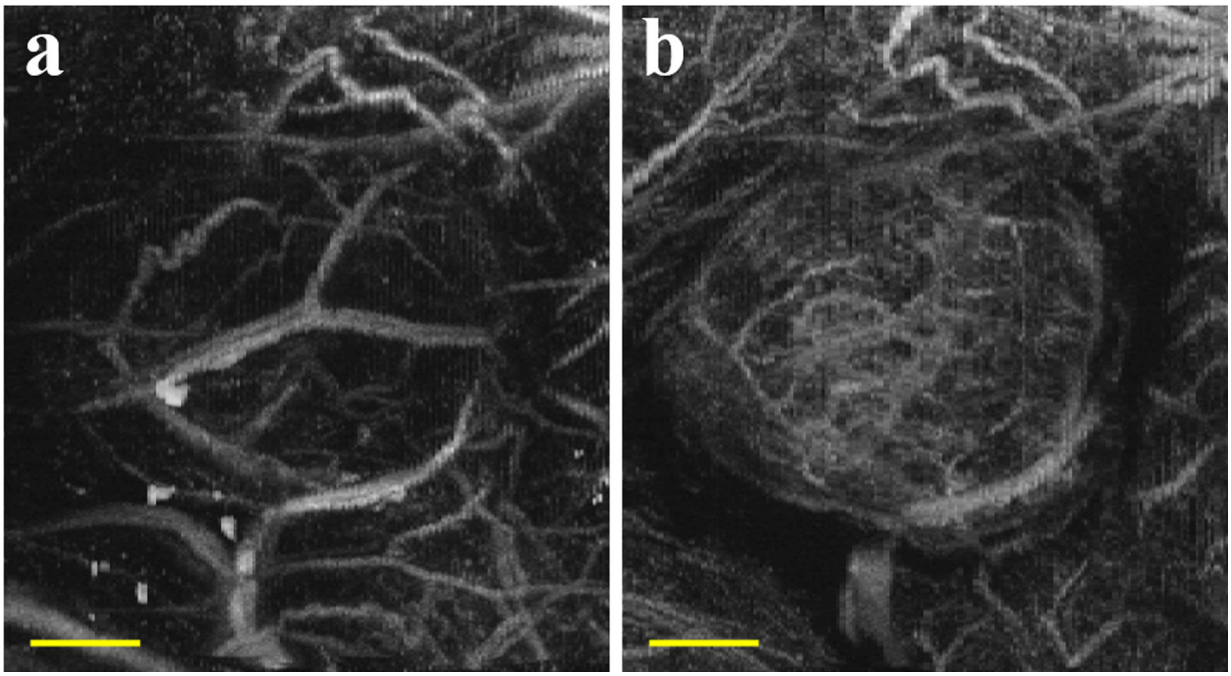

Figure 3:
Acoustic angiography maximum intensity projections of a rat fibrosarcoma tumor at a) 1200 kPa and b) 560 kPa. Scale bar = 4 mm.

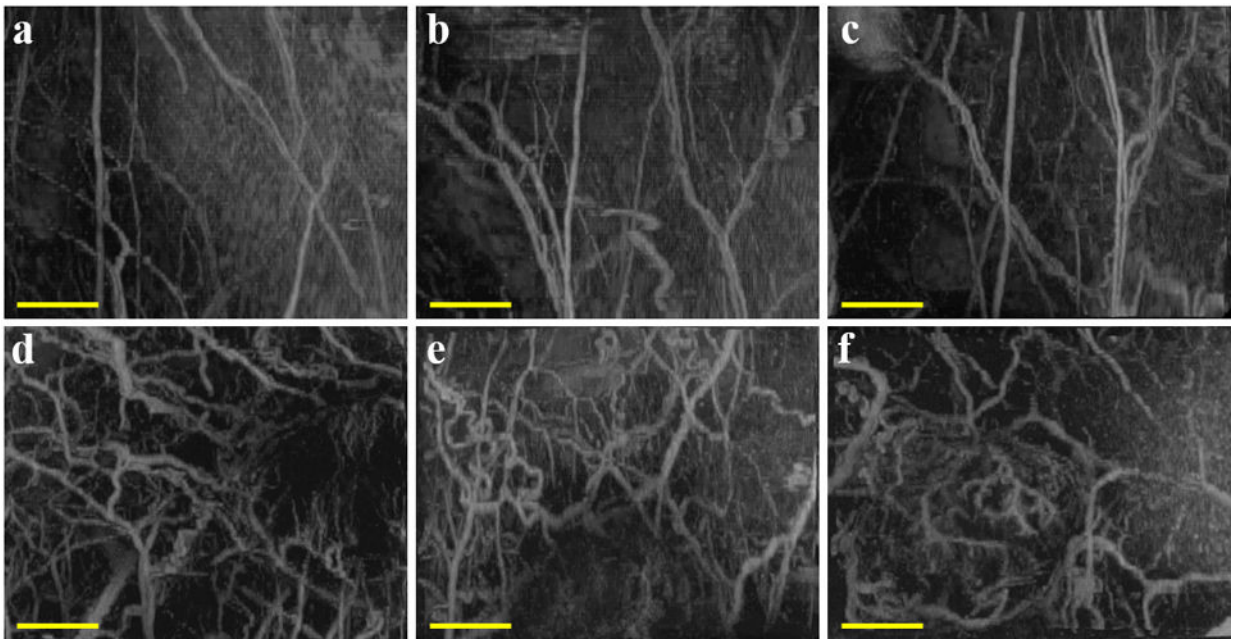

Figure 4:

Acoustic angiography maximum intensity projections showing microvasculature in healthy (a – c) or tumor-bearing (d – f) tissue in a subcutaneous rat fibrosarcoma model. Scale bar = 5 mm. Reprinted by permission from: Gessner RC, Aylward SR, and Dayton PA, Radiology, 2012;264:733–740, Radiological Society of North America.

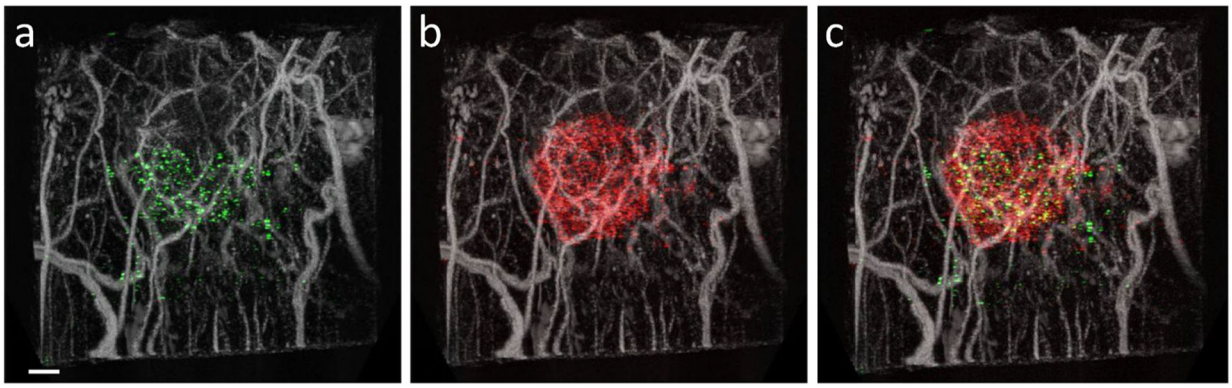

Figure 5:

Combined acoustic angiography and molecular imaging scans showing microvasculature and distribution of a) VEGFR2 (green), b) P- and E-selectins (red), and c) both VEGFR2 and P- and E-selectins in a subcutaneous rat fibrosarcoma tumor. Scale bar = 2 mm. Reprinted by permission from: World Molecular Imaging Society, Molecular Imaging and Biology, Lindsey BD, Shelton SE, Foster FS, and Dayton PA, 2016.

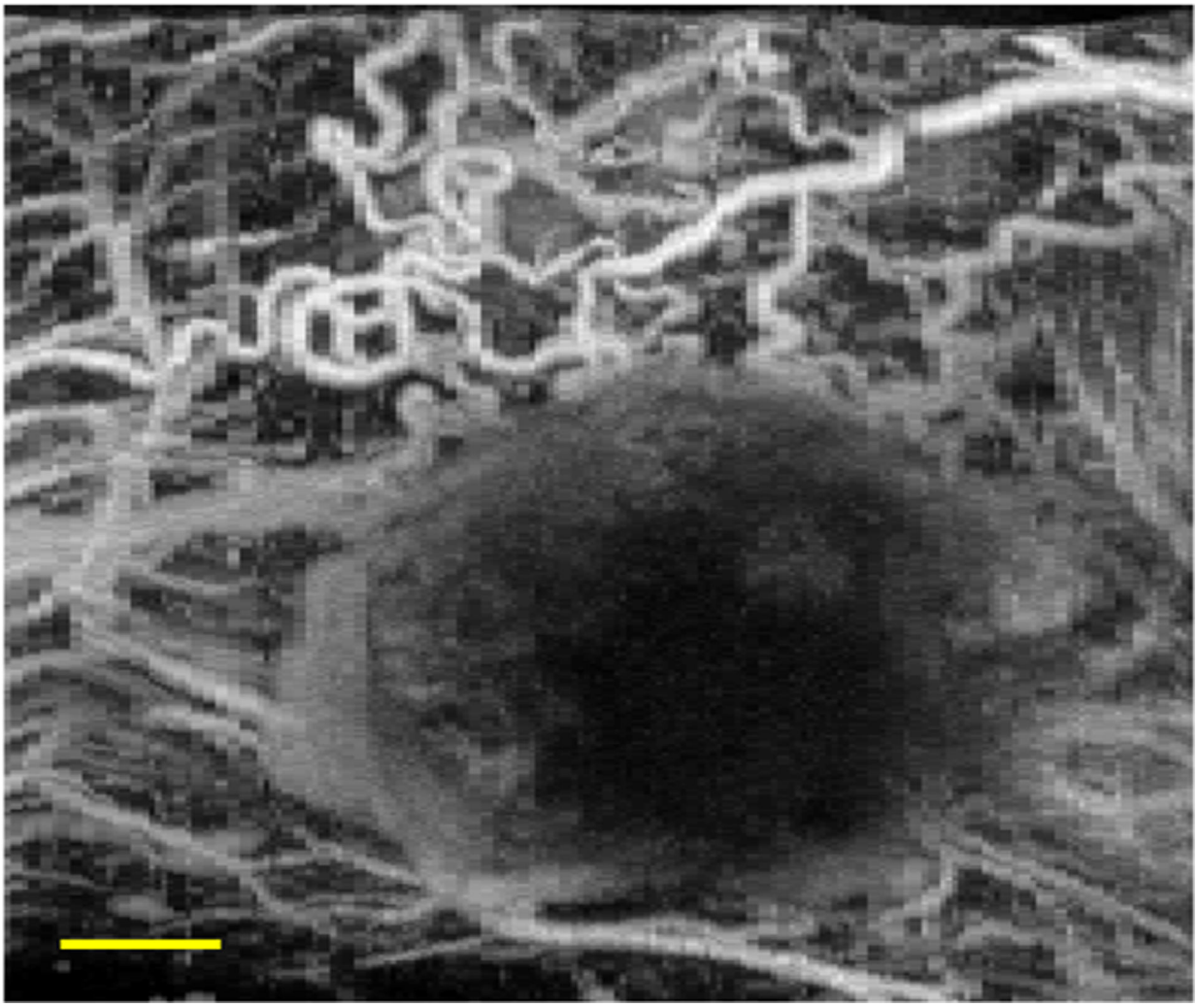

Figure 6:
Acoustic angiography maximum intensity projection of microvasculature surrounding a human lung tissue implant in a mouse flank. Scale bar = 3 mm.